JAEA-Technology
2007-003

JP0750130

Development of the Unattended Spent Fuel Flow Monitoring Safeguards System (UFFM) for the High Temperature Engineering Test Reactor (HTTR) (Joint Research)

Shigeaki NAKAGAWA, Masayuki UMEDA, David H. BEDDINGFIELD*
Howard O. MENLOVE* and Kiyonobu YAMASHITA

Department of HTTR
Oarai Research and Development Center

February 2007
Japan Atomic Energy Agency
日本原子力研究開発機構

JAEA-Technology

本レポートは日本原子力研究開発機構が不定期に発行する成果報告書です。
本レポートの入手並びに著作権利用に関するお問い合わせは、下記あてにお問い合わせ下さい。
なお、本レポートの全文は日本原子力研究開発機構ホームページ（http://www.jaea.go.jp/index.shtml）より発信されています。このほか財団法人原子力弘済会資料センター*では実費による複写頒布を行っております。

〒319-1195　茨城県那珂郡東海村白方白根2番地4
日本原子力研究開発機構　研究技術情報部　研究技術情報課
電話 029-282-6387, Fax 029-282-5920

*〒319-1195　茨城県那珂郡東海村白方白根2番地4　日本原子力研究開発機構内

This report is issued irregularly by Japan Atomic Energy Agency
Inquiries about availability and/or copyright of this report should be addressed to
Intellectual Resources Section, Intellectual Resources Department,
Japan Atomic Energy Agency
2-4 Shirakata Shirane, Tokai-mura, Naka-gun, Ibaraki-ken 319-1195 Japan
Tel +81-29-282-6387,　Fax +81-29-282-5920

Development of the Unattended Spent Fuel Flow Monitoring Safeguards System (UFFM) for the High Temperature Engineering Test Reactor (HTTR) (Joint Research)

Shigeaki NAKAGAWA, Masayuki UMEDA, David H. BEDDINGFIELD*,
Howard O. MENLOVE* and Kiyonobu YAMASHITA+

Department of HTTR
Oarai Research and Development Center
Japan Atomic Energy Agency
Oarai-machi, Higashiibaraki-gun, Ibaraki-ken

(Received January 4, 2007)

As of the safeguards approach in the HTTR facility, an unattended spent fuel flow monitor (UFFM) was developed to carry out an item counting of spent fuel blocks. The UFFM is so designed and fabricated as to be the compact and unique monitor system to verify a movement of spent fuel blocks in "difficult to access" area and reduce inspection efforts. The UFFM was well-incorporated in small space along fuel transfer path. This system consists of two detector packages, electronics named GRAND and computer. One package consists of two ionization chambers and a He-3 counter. Tungsten collimators are installed on the nose of the packages to increase the time difference between two detectors.

The IAEA acceptance tests were performed and it was confirmed the followings:

- All the detectors used in the UFFM were functioning properly to measure a spent fuel block flow.
- The time difference between detector signals was sufficient to determine the direction of the spent fuel blocks.
- The UFFM was useful to carry out the item counting of spent fuel blocks.

The UFFM was approved as the IAEA safeguards equipment applied the item counting for spent fuels in the safeguards approach in the HTTR.

Keywords: HTGR Fuel, HTTR, Safeguards Approach, Spent Fuel Flow Monitor

---

This report is the outcome of the joint development and application of the unattended spent fuel flow monitor for the HTTR under the agreement between the United States Department of Energy (DOE) and the JAEA. The JAEA has developed the UFFM in collaboration with the Los Alamos National Laboratory (LANL) through the DOE.

+ Department of Research Reactor and Tandem Accelerator, Nuclear Science Research Institute, Tokai Research and Development Center

* Los Alamos National Laboratory

高温工学試験研究炉（HTTR）の保障措置に用いる

使用済燃料フローモニターの開発

(共同研究)

日本原子力研究開発機構　大洗研究開発センター
高温工学試験研究炉部
中川　繁昭、梅田　政幸、David H. BEDDINGFIELD*、Howard O. MENLOVE*、山下　清信+

(2007年1月4日受理)

HTTRの保障措置手法において、使用済燃料ブロックの員数勘定を実施するために非立会型の使用済燃料フローモニターを開発した。使用済燃料フローモニターは、「接近困難な」場所にある使用済燃料ブロックの移動を非立会で検認できるようにし、査察業務量を減らせるようにした。設計・製作を工夫し、燃料ブロックの移動経路に沿った狭い空間にうまく組み込んだ。使用済燃料フローモニターは、２組の検出器管、GRANDと呼ばれる電子機器及びコンピュータから構成する。１組の検出器管は２つの電離箱と１つHe-3中性子計数管を収納している。また、２組の検出器管からの信号変化の時間遅れが大きくなるように、検出器管の先端に形状に工夫を加えたタングステン製のコリメータを設置した。

IAEAの受入検査を実施し、使用済燃料フローモニターが使用済燃料ブロックを検知するために十分な機能を有していること、信号変化の時間遅れが使用済燃料ブロックの移動方向を決定するために十分であることを示した。使用済燃料フローモニターについては、HTTRの使用済燃料ブロックの員数勘定を実施するために有効であることが確認され、IAEAの保障措置機器として承認された。

本報告書は、米国エネルギー省（DOE）と原子力機構の協定の下で実施された「高温工学試験研究炉（HTTR）の使用済燃料体の移動を検認する燃料カウンタ（UFFM）の共同開発と適用」の成果である。原子力機構は、米国ロスアラモス国立研究所と協力してUFFMを開発した。

大洗研究開発センター：〒311-1393　茨城県東茨城郡大洗町成田町4002
+　東海研究開発センター原子力科学研究所研究炉加速器管理部
*　米国ロスアラモス国立研究所

Contents

目　次

This is a blank page.

1. Introduction

The Japan Atomic Energy Agency (JAEA) has constructed the HTTR since March 1991. The first criticality was attained on November 10, 1998. The reactor core was filled fully with 150 fuel blocks in December 1998. The full power operation was achieved with the reactor outlet coolant temperature of 850 °C and 950 °C in 2001 and 2004, respectively.

The objectives of the HTTR are to establish and upgrade the technology basis for the high temperature gas-cooled reactor (HTGR) and develop the technology for high temperature heat applications [(1)]. The HTTR is a HTGR type research reactor with thermal output of 30 MW and outlet coolant temperature of 950 °C, employing low-enriched uranium fuels and helium gas as primary coolant. The major specifications of the HTTR are summarized in Table 1.1. All the fuel blocks burned up in the reactor core are refueled with the fresh fuel at the same time after every burn-up cycle. The average fuel burn-up reaches 22 GWday/t in the whole core (after three years with the facility availability of 60%). The total amount of Pu in the spent fuel blocks becomes about 6.5 kg after one burn-up cycle [(2)].

In the safeguards at the reactor facility, the item counting of fuel is required. The item counting in the light water reactor (LWR) is carried out visually, and all fresh and spent fuels can be verified in the fuel pond. On the other hand, nobody can see directly any spent fuel block in the HTTR facility. All fuel blocks are handled inside the vessel with shielding such as reactor pressure vessel (RPV), fuel-handling machine (FHM) or fuel storage rack due to high radiation from spent fuel and no functioning of helium as shielding material like water. This situation makes impossible for inspectors to carry out visual item counting for fuel blocks. Therefore, monitoring the movement of spent fuel blocks from reactor core was necessary to carry out the item counting for fuel blocks. The detection of spent fuel flow is very important information for the safeguards of the HTTR. Additionally it takes about 90 days to refuel all fuel blocks in the reactor core. This causes an increase of inspection effort if the inspector has to observe the movement of all fuel blocks. For the above-mentioned reasons, the use of the unattended spent fuel flow monitor (UFFM) was necessary to verify the spent fuel movement in the safeguards approach of the HTTR [(2)]. The unattended monitor has been installed at the door-valve (DV) between the RPV and the FHM during refueling. All spent fuel blocks inevitably pass through the DV at that time. Two detector packages are inserted into penetrations in the DV casing. The detection of the spent fuel block flow is determined from the time difference between the signals of them. The followings should be considered to design the UFFM:

- There is only limited space to install the detector package because the diameter of each penetration is 100 mm and the thickness of the DV casing is 560 mm.
- The distance between two packages is only 200 mm and the movement speed of fuel block during going through the DV is ~40 mm/s in maximum. It is difficult to determine the direction of the spent fuel block due to short time difference of ~5 sec from the signals.

To solve such problems, compact and unique detector package was designed. Each package has a tungsten collimator on the nose to make clear the time difference between the two detector packages. The tungsten collimator will also provide an asymmetric shape of profile for the transfer data to distinguish upward fuel transfer from downward transfer.

Three steps of the acceptance tests were performed to confirm the performance of the UFFM. In the phase-I-acceptance test in 1997, the fundamental function of detectors was confirmed at the laboratory. In the phase-II-acceptance test in 1998, the function of the UFFM as a whole system was confirmed after installation to the HTTR facility. The phase-III-acceptance test in 2000 and 2002 was performed as a final test to obtain IAEA authentication at the radioactivity measurement of some spent fuel blocks loaded in the HTTR. From the result of these acceptance tests, it was confirmed that the UFFM has a sufficient function to verify the direction of spent fuel block flow.

This report presents a design of UFFM for the HTTR facility and the results of performance tests. This project has been performed as joint development and application of the unattended spent fuel flow monitor for the HTTR under the agreement between the United States Department of Energy and the JAEA. The JAEA has developed the UFFM in collaboration with the Los Alamos National Laboratory (LANL). After authentication, the UFFM has become the property of the International Atomic Energy Agency (IAEA) through the Japan Support Programme for Agency Safeguards (JASPAS).

2. Necessity of UFFM in the HTTR safeguards

Cutting view of HTTR is shown in Fig. 2.1. The reactor core, 2.9 m in height and 2.3 m in diameter, consists of 30 fuel columns. Each fuel column consists of 5 fuel blocks stacked vertically. The reactor core consists of 150 fuel blocks with 12 different uranium enrichments to optimize the power distribution. The uranium enrichment ranges from 3 up to 10 wt%. The top, side and bottom replaceable reflector blocks surround the reactor core. Sixteen pairs of control rods are inserted into control rod guide column in the reactor core and side reflector regions. The permanent reflectors surround the side replaceable reflectors and are fixed by the core restraint mechanism.

The structure of the fuel block is shown in Fig. 2.2. The fuel block consists of a graphite block and fuel rods. A fuel rod contains 14 fuel compacts in which coated fuel particles are dispersed. A coated fuel particle consists of UO_2 kernel coated with three pyro-carbon layers and a SiC layer. The fuel rods are inserted into coolant holes of fuel blocks. A fuel block contains 31 or 33 fuel rods. The weight of one fuel block is about 100 kg. The uranium enrichment of each compact is the same in a fuel block.

The fuel blocks are transferred with the FHM among the reactor core, fresh fuel storage and spent fuel storage. Figures 2.3 and 2.4 show a movement path of the fuel blocks in the HTTR. The refueling procedure in the HTTR is as follows:

1. The spent fuel blocks are unloaded from the reactor core into the FHM through the DV. The FHM has a long arm with a gripper to enter the reactor core through the standpipes at the upper hemisphere of RPV (See Fig. 2.1). The gripper is inserted into the fuel handling hole at the center of the fuel block (See Fig. 2.2). Then the gripper holds and lifts it. Five spent fuel blocks and two reflector blocks as one column are removed at the same time. The FHM containing spent fuel blocks is transferred with the ceiling crane. The DV is used as an attachment between the reactor

and FHM. Figure 2.5 shows the exterior of FHM and DV.

2. The FHM is transferred from the reactor core to the spent fuel storage. The spent fuel blocks are swept out from the FHM into the rack.
3. The FHM is transferred from the spent fuel storage to the fresh fuel storage to fill with fresh fuel blocks.
4. The FHM is transferred from the fresh fuel storage to the reactor core. The fresh fuel blocks are loaded from the FHM into the space where the spent fuel blocks are just removed before in the reactor core.
5. The FHM unloads spent fuel blocks in another column. (to the procedure 1.)

The upper hemisphere of the RPV cannot be removed to handle the fuel block easily because the radiation from the reactor core cannot be shielded. All fuel blocks are handled inside the facility equipment as mentioned above. Nobody can see any fuel blocks during refueling. As spent fuel blocks are in the "difficult to access" area, a direct visual verification for item counting of them cannot be applied in the HTTR. All spent fuel blocks in the reactor core are refueled every three years. It takes about 90 days to refuel them with the FHM because of the slow speed of the FHM movement by the ceiling crane. The weight of the FHM is about 150 ton.

From the above-mentioned reason, the UFFM must be applied in the HTTR safeguards approach. The UFFM can reduce the inspector's efforts using its unattended monitoring performance.

3. Outline of UFFM

The design goals of the UFFM for the HTTR included (1) to measure the number of spent fuel blocks and (2) to determine the direction of spent fuel block transfers. To accomplish these goals, the UFFM is so designed as to have short and long ionization chambers (ICs) for the gamma-ray measurements and He-3 counter for the neutron measurements [(3)]. The schematic diagram of the UFFM is shown in Fig. 3.1. One He-3 counter and two ICs are included in the detector package. Two detector packages placed along a transfer path of fuel blocks make possible to determine the direction of spent fuel block. The signals from detectors send to the GRAND of electronics and computer with software to obtain the data of spent fuel block transfers. The spent fuel block transfers can be identified when neutron and gamma ray are detected at the same time. If only gamma ray is detected, the irradiated specimen transfer is considered. The photo of two detector packages of the UFFM installed in the penetration of the DV is shown in Fig. 3.2. The photo of the cabinet contained the GRAND and the computer is shown in Fig. 3.3.

Figure 3.4 shows a cross-sectional view of the detector package of the UFFM. Table 3.1 shows detector specifications of the UFFM. The short and long ICs contain xenon gas and are designed to measure gamma dose in the range of 0.1 to 10^6 R/h from the fuel block. The short IC is near the spent fuel block and the long IC is placed behind it. He-3 counter is located at the back of tungsten and lead shielding to reduce the gamma dose. The fill-pressure of the He-3 counter is 4 atmospheres of ^{3}He plus CO_2. The long IC and He-3 counter are set in a polyethylene cylinder to fix their position and to moderate the neutrons. All the detectors are positioned 40-50 cm from the centerline of the fuel transfer hole and perpendicular to the axis. They are designed to be compact because of a limited space and their effective lengths are shorter than that for conventional detectors.

Normally, U-235 fission chambers are used to measure neutrons from spent fuel because of the pulse pile-up interference from the intense gamma-ray dose. For the UFFM for the HTTR, He-3 counter placed iron and tungsten shielding to reduce the gamma dose at the counter location is used. The He-3 counter provides about two orders of magnitude more efficiency for neutron detection than for fission chamber. This added sensitivity allows the detection of neutrons from low burn-up fuel. The He-3 counter has a special design to allow neutron counting in gamma-ray fields as high as 100 R/h.

Two ICs include a high sensitivity IC in the nose of the detector package adjacent to the spent fuel block as well as a longer IC shielded by iron and tungsten behind the short IC. The two ICs cover a gamma detection range of about eight orders of magnitude and they provide redundancy in case of component failure. Because the maximum distance between the two detector packages is only 200 mm and the fuel blocks transfer on a path is about 400 mm from the detector packages, it is difficult to resolve the direction of spent fuel block from the time difference between two detectors. Tungsten collimator is placed on the nose of the detector package to provide more definitive resolution for transfer direction. This tungsten collimator allows the followings:

- To increase the time difference between two detectors,
- To provide an asymmetric shape for the transfer data peak profile to distinguish upward fuel transfer from downward transfer.

The stainless steel detector package is sealed hermetically, and has a length of 560 mm and a maximum diameter of 100 mm.

The tungsten collimator on the nose of detector package improves the resolution to obtain the direction of spent fuel block. The collimator of the upper detector package opens a window to upper side and that of the lower one to lower side. When a spent fuel block passes through the transfer path in the DV, such signals as shown in Fig. 3.5 will be expected. The movement direction can be identified from signal time difference between two detector packages. Tungsten shielding at the intermediate and back position of detector package has a function to reduce a dose rate to the operator around the DV.

During the reactor operation, the UFFM will be disconnected from the GRAND and a long He-3 counter inside the cabinet will be connected to the GRAND to check the electronics performance and room background as shown in Fig. 3.6. The long He-3 counter provides assurance to the inspectors that the electronics are functional during 3 years period between spent fuel discharges.

4. Performance tests for UFFM

4.1 Phase-I-acceptance test

Phase-I-acceptance test was performed at the LANL to confirm basic monitor characteristics and to obtain proper setting for the monitor by using ^{226}Ra gamma ray and ^{252}Cf neutron sources. The cable between the detector package and the GRAND was 50 m long to check possible attenuation of the signal.

The plateau curve of the He-3 counter is shown in Fig. 4.1 where the total counting rate is plotted as a function of the high-voltage bias. The gamma ray is measured as a noise when the He-3 counter measures neutrons from a spent fuel block. Figure 4.2 shows the measured response profiles for He-3 counter when the neutron source was moved on an axis where the spent fuel block is transferred. The figure shows that the offset in the initial rise of the response indicated the direction of spent fuel block. The shadowing effect of shielding to the position of the neutron source causes the multiple peaks on the profiles because the tungsten shielding is placed in front of the He-3 counter and the detector packages are in the air.

Test measurements were performed to determine the sensitivity of the UFFM to fresh fuel transfer. Ten PWR fuel rods to simulate a fresh fuel of the HTTR were placed at a distance of 50cm from the front of the UFFM to determine the sensitivity to the gamma ray and neutron from the fresh fuel. Gamma-ray count rate was too small to be recorded. There is no possibility to detect the loading of fresh fuel into the reactor core.

The two ICs are used for measuring the relative gamma-ray dose. The short IC is near the sample and the long IC is shielded by about 20cm of steel and tungsten as shown in Fig. 3.4. Thus, the short IC will be several orders of magnitude more sensitive than the long IC. The IC response is proportional to the gamma source strength. Figure 4.3 shows the IC response as a function of distance from the 1500 R/h ^{226}Ra source which is simulated the spent fuel block. The gamma dose at the design-basis distance of 20cm reaches to about 60 R/h and the short IC signal shows about 15 cps. As it was expected that the background noise would be 1~2 cps, the IC sensitivity is several orders of magnitude above the background noise level. The two ICs in each detector package are used to provide redundant data on the direction of motion and speed of the fuel block transfers.

From the above-mentioned results, the following were confirmed:

- All the detectors used in the UFFM are functioning properly.
- The He-3 counter can measure neutrons from a spent fuel block separating a gamma-ray pile-up as a noise.
- Verification for fresh fuel blocks loading to the reactor core is not possible in the HTTR.

4.2 Phase-II-acceptance test

Phase-II-acceptance test was performed at the HTTR site to confirm the performance of the UFFM installed the DV. In the phase-II-acceptance test, the neutron profile measurements were performed using an Am-Be neutron source (NS).

Figure 4.4 shows the schematic cross-sectional view of the NS used in the profile measurements of axial and radial neutron responses. This NS has an intensity of 1×10^7 n/s and is stored in the stainless steel container. That container has a dimension of 216 mm diameter and 312 mm height similar to a fuel block. The stainless steel and polyethylene shielding surround the NS in the container. The position of the container including the NS was changed from -180cm to +180 cm in the vertical direction along the fuel path around the DV. Then the container is moved from –20 cm to +20 cm in the radial direction at the position to get a maximum neutron count rate.

Figure 4.5 shows the response profile of He-3 counter to vertical movement of the NS. The direction of spent fuel block can be identified using the time difference between the monitor A (upper side) and B (lower side) in the signal profile or by using the shape of transfer pattern. The monitor B responded first as the NS was transferred upward below the DV. The maximum difference of profiles A and B is approximately 40 cm despite detector pitch of 20 cm because the monitor A is more shielded than the monitor B due to the concrete and the door-valve casing. The maximum signal of the upper and lower He-3 counters are equal because both counters are located in the symmetric arrangement. In the actual refueling procedure, the clear difference of profiles A and B in the upper region of the door-valve will be expected because the fuel handling machine is located on the door-valve. For the normal fuel transfer speed of about 1cm/s, this 40 cm offset represents about 40 seconds of time difference in the graphical display of the peak. In this measurement, there are no multiple peaks on the profiles observed in the phase-I-acceptance test because the UFFM is placed at the real configuration. When a count rate relation changes from $n(A)<n(B)$ to $n(A)>n(B)$, spent fuel block moves upwards, that is, from core to the FHM. The n(A) and n(B) are count rate of each He-3 counter. If the relationship would change from $n(A)>n(B)$ to $n(A)<n(B)$, spent fuel block moves downwards, that is, from the FHM to core. But this movement direction is highly improbable in normal refueling sequence in the HTTR. According to the measurement result, the difference in count rates measured by the monitor A and B is clearly bigger when the NS is located below the DV than the NS is located above the DV. That reason is that the neutron transports to the DV without attenuation in the air when the NS located above it. On the other hand, the neutron transports through the floor concrete and the DV casing when the NS located below. The neutron attenuation in the floor concrete makes the signal difference clear. In the case of actual refueling, the signal difference between two monitors will be clear independently of fuel location around the DV because the FHM containing the shielding. To evaluate the neutron transfer pattern using continuous motion and software of data collection, the NS was moved at a speed of about 1 cm/s. The detection time bin in the GRAND was set at 2 seconds. The NS was moved from 180 cm above the detectors-center line to 180 cm below. The direction of the crane was then reversed to pull the NS up through the UFFM to provide data for both directions motion. The transfer data profile is shown in Fig. 4.6. The time difference between neutron signals shows the movement direction. The result of measurement shows that the offset in the initial rise of the response indicates the speed and direction of the spent fuel block.

4.3 Phase-III-acceptance test

(1) Fuel movements

There have been two fuel movement activities at the radioactivity measurement in the HTTR performed during the early operation of the reactor. The first fuel movement occurred October 31 to November 15, 2000 [(4)] and the second fuel movement occurred from October 17 to November 9, 2002 [(5)]. Both of these activities were experiments performed to confirm core power distribution calculations. The fuel exposure at the time of the year 2000 activity was 280 MWd/t, very low. At the 2002 activity the average exposure was 4600 MWd/t, still quite low. The maximum fuel exposure in the HTTR is expected to reach to 22000 MWd/t in average. Both fuel movement activities examined the same fuel columns. The location of the measured columns is shown in Fig. 4.7. Each fuel column is composed of five vertically stacked block layers. There are four distinct fuel column types (zones) distributed over the core to provide uniform burn-up. The columns are distinguished by different initial enrichments. Boron is present in the fuel as a burnable poison and is distributed vertically in the core as shown in Table 4.1. In the experiments, one column of each of the four types was examined. Table 4.1 lists the characteristics of each column type.

The year 2000 fuel movement declarations are listed in Table 4.2. Because the fuel movements naturally occurred in four distinct time periods, four references to the movement activity clusters have been generated. Each referenced movement is shown in a graphic captured from the Radiation Review software and are presented in Fig. 4.8 and 4.9. Within each referenced movement the individual fuel transfers are readily distinguished [(6)].

The year 2002 fuel movement declarations are listed in Table 4.3. The fuel movements have again been broken into temporally related movement references. Each referenced movement is shown in a graphic captured from the Radiation Review software presented Fig. 4.10 and 4.11. Within each referenced movement the individual fuel transfers are readily distinguished [(6)].

(2) Discussion

All of the fuel movements listed in the declarations provided in Tables 4.2 and 4.3 are clearly identified as shown in Figs. 4.8-4.11. This is extremely encouraging because the fuel had only a 4600 MWd/t exposure (Max. 22000 MWd/t after full burn-up) in 2002 and a considerably lower exposure in 2000. Despite the low exposure level of the fuel, all of the movements in both experiments are clearly identifiable. Furthermore, the ability to identify discrete fuel movements was verified enough to identify an apparently undeclared fuel movement.

When examining the data from the fuel movements, it becomes apparent that there is a consistent pattern to the data trace from the short ion chamber channel of both units of the UFFM system that is indicative of the direction-of-motion of the individual activities. The original scheme to determine the direction of motion of the individual fuel blocks was to examine the timing differences between the monitor A and monitor B signal maximum for a particular detector. In this scenario an outbound assembly can be identified by the lower monitor B detector maximum appearing prior to the upper monitor A maximum. Scrutiny of the data indeed demonstrates that the timing difference provide a reliable direction-of-motion indication. However, the timing differences are small (due to the close relative positioning of the two monitors) and the discrete shape of the data in the Short Ion Chamber data channels provides a more easily discernable indication of the direction of motion. Figure 4.12 shows this shape for outbound and inbound fuel blocks from recorded data. From Fig. 4.12, the direction of motion is evident by the relative ordering of the three major features of a fuel movement. For fuel removal from the core the features appear in the order, A-B-C and for exposed fuel replacement the ordering is reversed to C-B-A. This pattern is evident in all fuel movements where the fuel assembly was placed in the FHM for years 2000 and 2002 data. Because this shape is not changing with increasing burn-up, it is expected to be a reliable indicator throughout the life of the core.

Comparing the data from the year 2000 fuel movements with the year 2002 activity, the constancy of the data pattern in the short IC channel is evident. Also it is evident that there is yet to be much useful visual data from the neutron and long IC data channels. The neutron data and long IC data from the year 2000 measurements shows scatter typical of poor counting statistics due to the low count rate attributable to the very low burn-up level at that time. The year 2002 data represents the response to a core average of 4 GWday/t. The year 2002 data shows the flux profile of the reactor much more clearly than at the lower exposure. The long ion chamber and the He-3 neutron data will become visually useful for assessing fuel movements as the core exposure increases. The long IC channel was included in the HDVM to provide gamma-ray data in the event that the short IC channel saturated from the spent fuel. The long IC tube is approximately 1000 times less sensitive than the short IC tube in the HDVM unit. This sensitivity difference provides an overlapping operating range for the detectors. At low dose rates, the short IC is sensitive and the long IC does not provide useful data (the present case), at high dose rates both detectors provide useful gamma-ray measurement data, and at very high dose rates the short IC may saturate and the long IC provides useful data. If the gamma-ray production rate does increase enough to saturate the short IC channel, the long IC will certainly have enough signal to become visually useful for data review.

5. Conclusion

The UFFM was applied to carry out the item counting of spent fuel block in the HTTR safeguards approach. The UFFM has been installed at the DV where is only path for the spent fuel block from the reactor core. The UFFM was designed to measure the number of spent fuel blocks and determine the direction of those transfers. From the result of all the acceptance tests, it was confirmed that the UFFM is applicable to identify the spent fuel movement despite the short pitch between two detector packages. The number of spent fuel blocks and direction of transfers can be verified in the unattended mode. The direction of transfer can be determined from the time difference and the signal profile from each two monitors. The UFFM was approved as the IAEA safeguards equipment applied the item counting for spent fuels in the safeguards approach in the HTTR. The design concept and the measurement method of the UFFM would be applicable in the safeguards approach for the future advanced HTGR.

References

(1) S. SHIOZAWA, et al., "Overview of HTTR Design Features", Nucl. Eng. Des., 233, p.11-21 (2004).

(2) K. YAMASHITA, et al., "Safeguards Concept for the High Temperature Engineering Test Reactor Using Unattended Fuel Flow Monitor System", J. Nucl. Mater. Manage., XXV(4) (1997).

(3) H. O. MENLOVE, et al., "Spent Fuel Monitoring for International Inspection at the High-temperature Engineering Test Reactor", LA-UR-98-2377 (1998).

(4) N. FUJIMOTO, et al., "Measurement of Gamma Ray from Fuel of High Temperature Engineering Test Reactor -Method of Measurement and Results-", JAERI-Tech 2001-002 (2001). (in Japanese)

(5) N. NOJIRI, et al., "Power Distributions in the High Temperature Engineering Test Reactor (HTTR) by Measuring Gross Gamma Ray form the Fuel Assembles", JAERI-Tech 2003-086 (2003). (in Japanese)

(6) D. H. BEDDINGFIELD, "High-Temperature Engineering Test Reactor Door Valve Monitor System Review", LA-UR-03-2974 (2003).

Table 1.1 Major specifications of the HTTR

Thermal power	30 MW
Reactor core height	2.9 m
Reactor core diameter	2.3 m
Average power density	2.5 MW/m^3
Fuel block	Hexagonal
Number of fuel blocks	150
Fuel	UO_2
Fuel type	Coated fuel particle
Uranium enrichment	3 -10 wt%
Number of different uranium enrichments	12
Moderator	Graphite
Outlet coolant temperature	950 °C
Coolant pressure	4 MPa
Reactor pressure vessel	Steel
Coolant	Helium gas
Average fuel burn-up	22 GWd/t
Maximum fuel burn-up	33 GWd/t
Refueling	All fuel blocks for once
Refueling period	Every three years
^{235}U in reactor core	52kg
Pu after 660 burn-up days	6.5kg

Table 3.1 Detector specifications

Long IC	Model LND 52133 Diameter: 26mm, Length: 185mm Measurement range: 0.1~10^6R/h Sensitivity: 6.0×10^{-11}A/R/h Operating bias: -300V Xenon gas fill
Short ICs	Model LND 52134 Diameter: 25.4mm, Length: 125mm Measurement range: 0.1~10^6R/h Sensitivity: 6.0×10^{-11}A/R/h Operating bias: -300V Xenon gas fill
He-3 counter	Reuter-Stokes RS-P4-0803-103 (MG) Diameter: 25.4mm, Length: 76mm(active length) Measurement range: ~10^4nv Sensitivity: 10cps/nv Operating bias: 1680V He-3 gas fill PDT-110A Pre-amplifier

Table 4.1 ^{235}U initial enrichment and poison content of HTTR column types

Block Layer*	Initial ^{235}U Enrichment (wt%) and Total U loading (kg) by Fuel Zone Number							
	1		2		3		4	
1	6.66%	6.13kg	7.83%	6.20kg	9.34%	5.70kg	9.84%	5.77kg
2	5.20%	6.18kg	6.25%	6.14kg	7.16%	5.73kg	7.83%	5.84kg
3	4.28%	6.18kg	5.20%	6.20kg	5.89%	5.81kg	6.25%	5.78kg
4	3.30%	6.20kg	3.87%	6.17kg	4.28%	5.79kg	4.80%	5.86kg
5	3.30%	6.20kg	3.87%	6.17kg	4.28%	5.88kg	4.80%	5.85kg

* Layers listed from core top (1) to bottom (5)

Table 4.2 Fuel movement at the radioactive measurement in 2000 (After 280 MWd/t burn-up)

Fuel Column ID*	Fuel Block ID	Transfer Date & Time		Reference Number
		From reactor core	Into Reactor core	
B01	H001F1	10/31 0:57 PM	10/31 4:21 PM	1
	E007F1	10/31 1:18 PM	10/31 3:59 PM	
	C001F1	10/31 1:39 PM	10/31 3:38 PM	
	A001F1	10/31 2:00 PM	10/31 3:17 PM	
	A101F1	10/31 2:22 PM	10/31 2:54 PM	
C02	J004F1	11/1 0:19 PM	11/1 3:47 PM	2
	G004F1	11/1 0:42 PM	11/1 3:24 PM	
	E004F1	11/1 1:04 PM	11/1 3:01 PM	
	B004F1	11/1 1:27 PM	11/1 2:39 PM	
	B104F1	11/1 1:50 PM	11/1 2:54 PM	
D02	K203F1	11/14 1:44 PM	11/14 5:23 PM	3
	I203F1	11/14 2:08 PM	11/14 4:59 PM	
	F203F1	11/14 2:31 PM	11/14 4:35 PM	
	C203F1	11/14 3:00 PM	11/14 4:12 PM	
	C303F1	11/14 3:25 PM	11/14 3:47 PM	
D01	L202F1	11/15 0:23 PM	11/15 4:25 PM	4
	J202F1	11/15 0:48 PM	11/15 4:00 PM	
	G202F1	11/15 1:27 PM	11/15 3:34 PM	
	D202F1	11/15 1:52 PM	11/15 3:08 PM	
	D302F1	11/15 2:18 PM	11/15 2:42 PM	

*The location of each fuel column is shown in Fig. 4.7.

Table 4.3 Fuel movement at the radioactive measurement in 2002
(After 4600 MWd/t burn-up)

Fuel Column ID	Fuel Block ID	Transfer Date & Time		Reference Number
		Out of Reactor	Into Reactor	
D02	K203F1	10/17 10:44 AM	10/17 2:59 PM	5
	I203F1	10/17 11:05 AM	10/17 2:37 PM	
	F203F1	10/17 11:26 AM	10/17 2:16 PM	
	C203F1	10/17 11:47 AM	10/17 1:55 PM	
	C303F1	10/17 0:09 PM	10/17 1:32 PM	
D02	K203F1	10/18 10:38 AM	10/18 11:13 AM	6
	K203F1	10/18 11:24 AM	10/18 2:58 PM	
D02	K203F1	10/18 3:13 PM	10/18 6:22 PM	7
	I203F1	10/18 3:34 PM	10/18 6:00 PM	
	F203F1	10/18 3:55 PM	10/18 5:39 PM	
	C203F1	10/18 4:16 PM	10/18 5:18 PM	
	C303F1	10/18 4:38 PM	10/18 4:56 PM	
D02	K203F1	10/19 0:45 PM	10/19 1:31 PM	8
	K203F1	10/19 1:55 PM	10/19 2:15 PM	
	K203F1	10/19 6:01 PM	10/19 6:04 PM	
	K203F1	10/19 6:17 PM	10/19 7:26 PM	
D02	K203F1	10/20 11:18 AM	10/20 6:39 PM	9
	I203F1	10/20 1:31 PM	10/20 6:17 PM	
	F203F1	10/20 2:41 PM	10/20 5:56 PM	
	C203F1	10/20 3:49 PM	10/20 5:31 PM	
	C303F1	10/20 4:55 PM	10/20 5:13 PM	
D01	L202F1	10/21 11:28 AM	10/21 7:10 PM	10
	J202F1	10/21 1:45 PM	10/21 6:47 PM	
	G202F1	10/21 2:55 PM	10/21 6:24 PM	
	D202F1	10/21 4:07 PM	10/21 6:02 PM	
	D302F1	10/21 5:18 PM	10/21 5:38 PM	
B01	H001F1	11/8 11:22 AM	11/8 6:59 PM	11
	E007F1	11/8 1:50 PM	11/8 6:37 PM	
	C001F1	11/8 3:00 PM	11/8 6:16 PM	
	A001F1	11/8 4:05 PM	11/8 5:55 PM	
	A101F1	11/8 5:12 PM	11/8 5:33 PM	
C02	J004F1	11/9 11:10 AM	11/9 7:45 PM	12
	G004F1	11/9 1:41 PM	11/9 7:22 PM	
	E004F1	11/9 3:14 PM	11/9 7:00 PM	
	B004F1	11/9 4:33 PM	11/9 6:38 PM	
	B104F1	11/9 5:52 PM	11/9 6:15 PM	

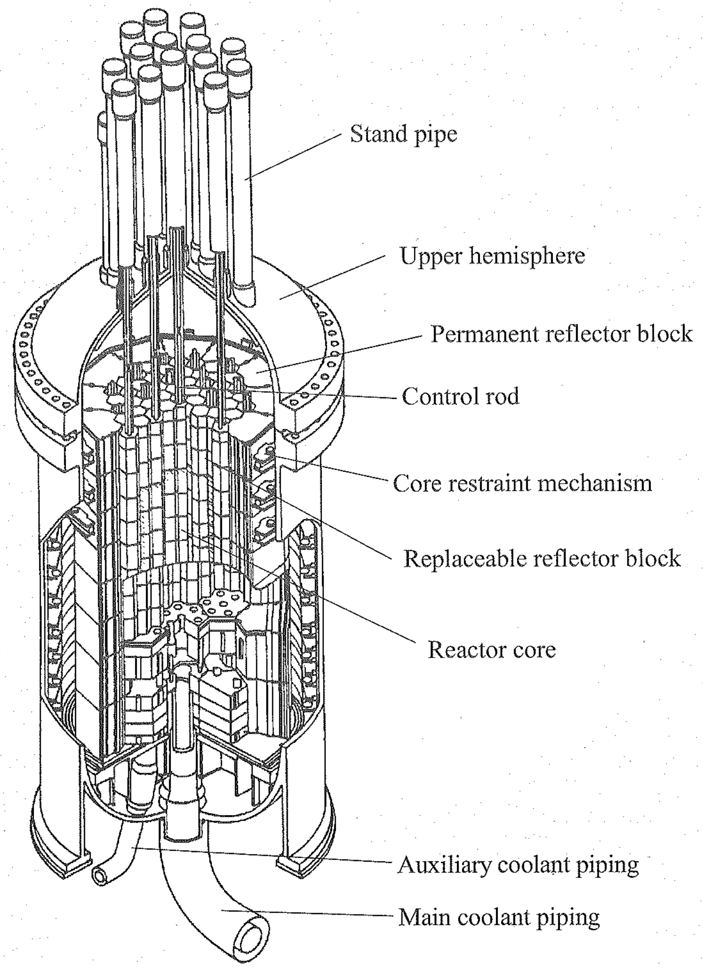

Fig. 2.1 Cutting view of reactor pressure vessel and reactor core of HTTR

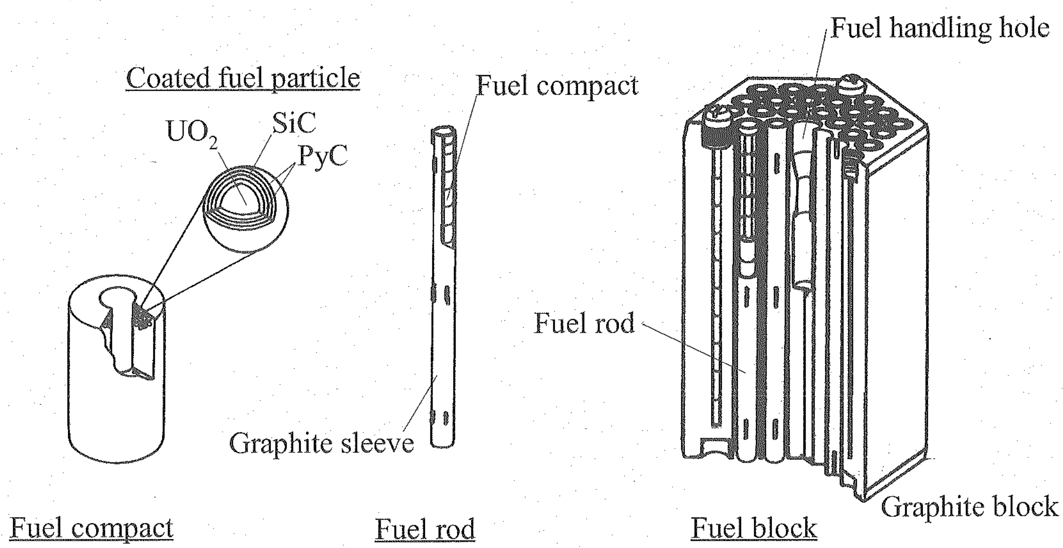

Fig. 2.2 Structure of fuel block

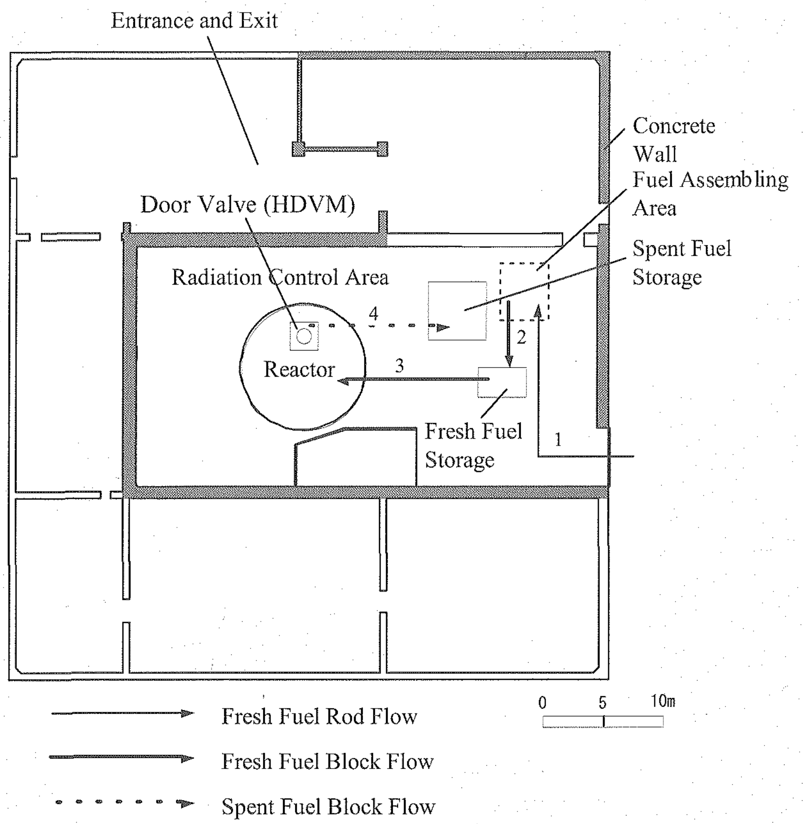

Fig. 2.3 Horizontal view of movement path of fuel block in the reactor building

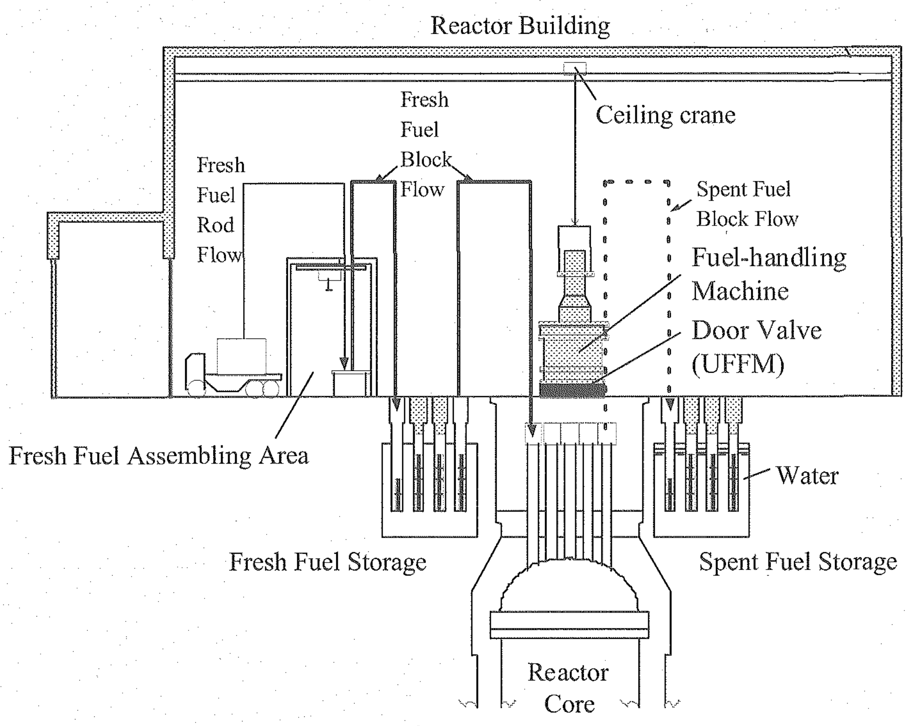

Fig. 2.4 Vertical view of movement path of fuel block in the reactor building

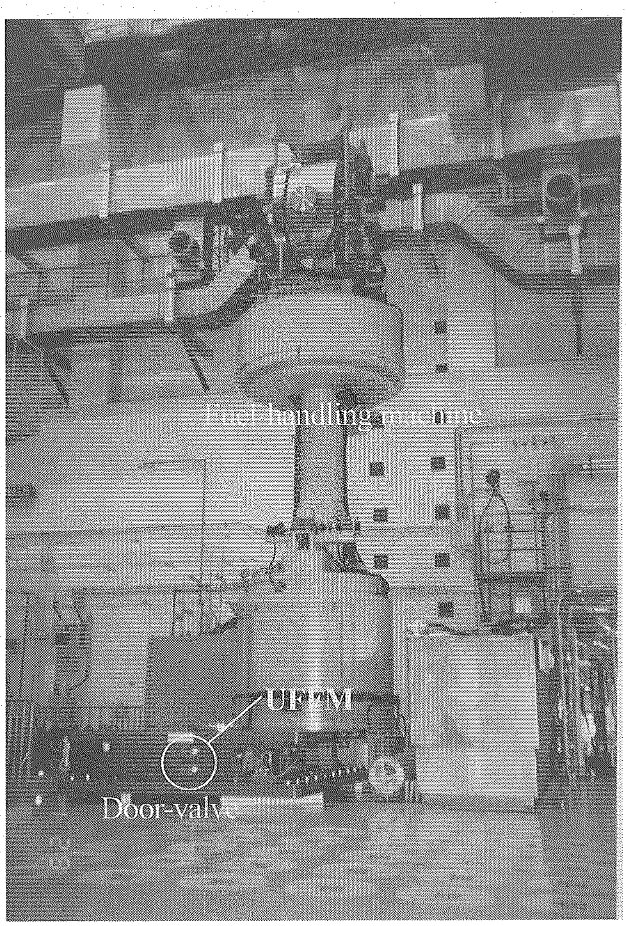

Fig. 2.5 Exterior of fuel-handling machine and door-valve

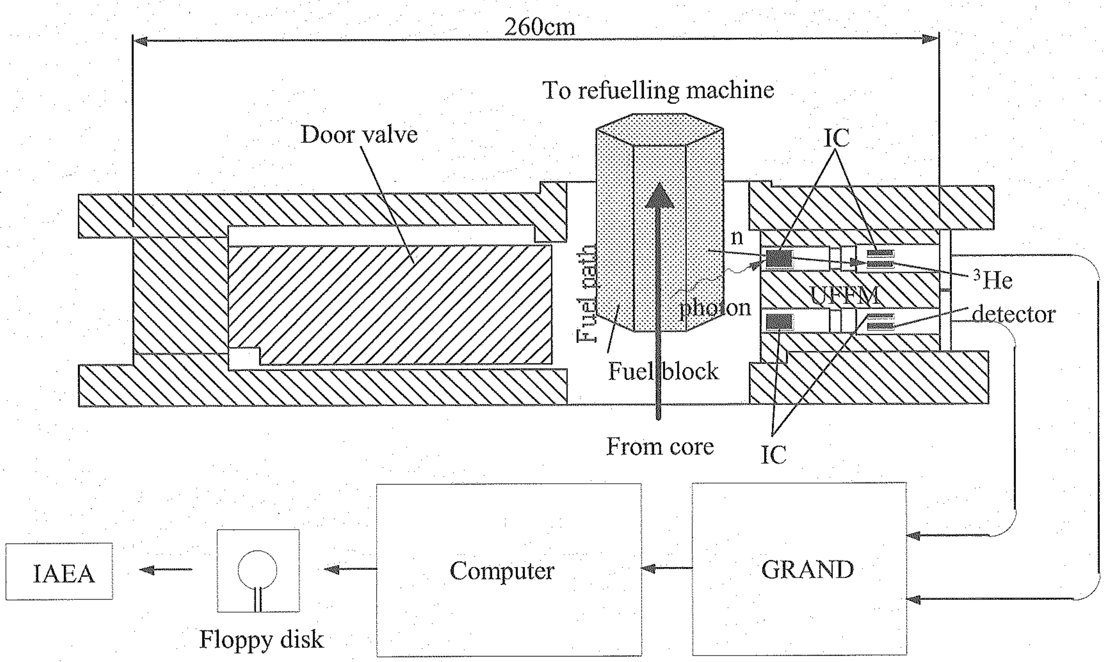

Fig. 3.1 Schematic diagram of the UFFM

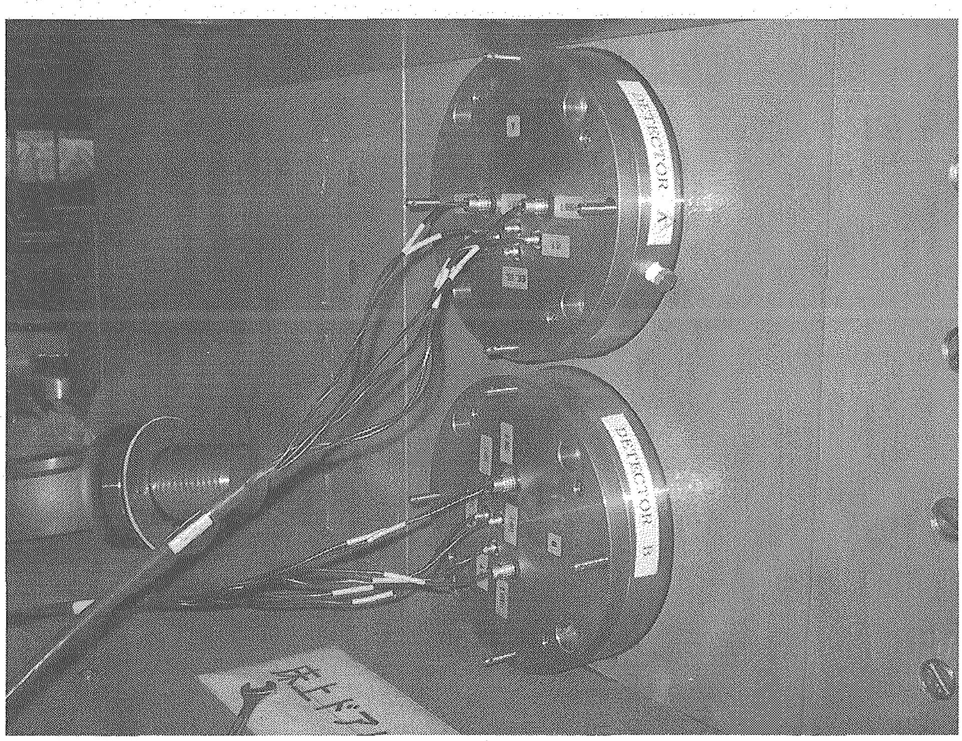

Fig. 3.2　Two detector packages of the UFFM installed in the penetration of the DV

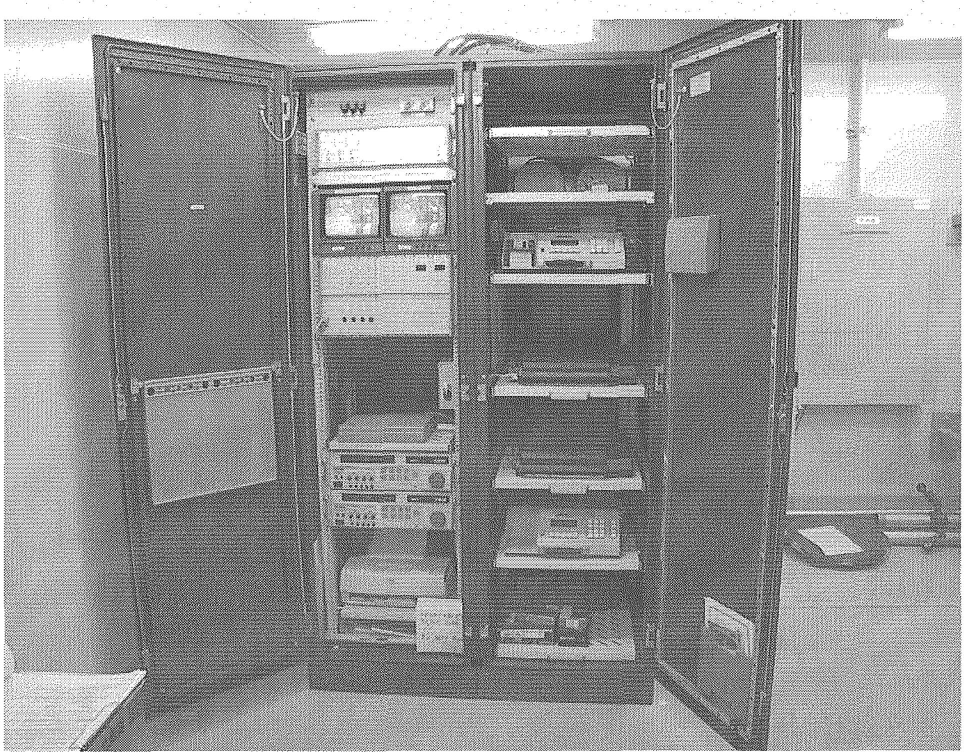

Fig. 3.3　Cabinet contained the GRAND and the computer

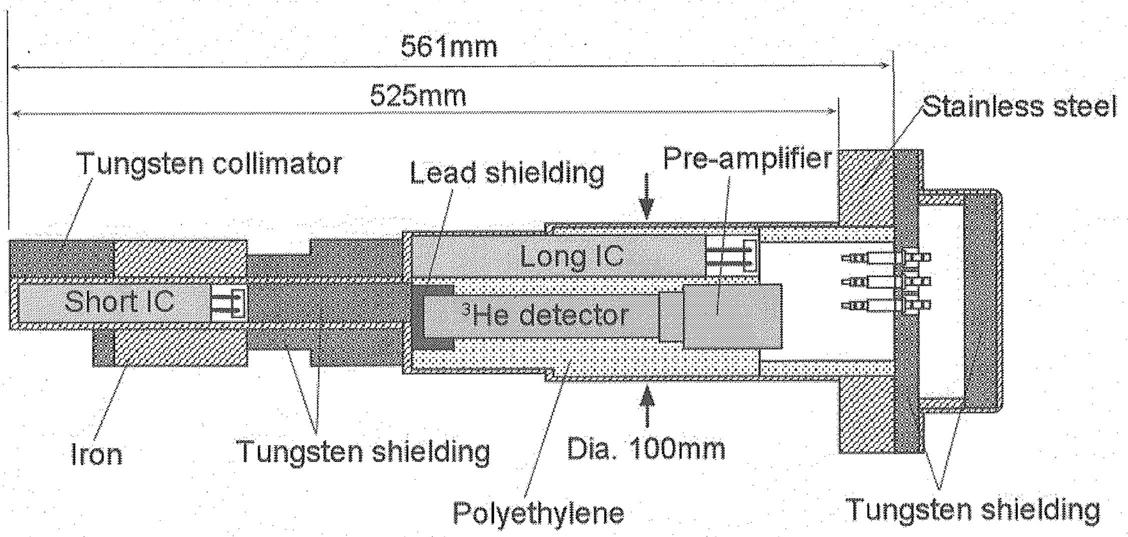

Fig. 3.4 Cross-sectional view of detector package of UFFM

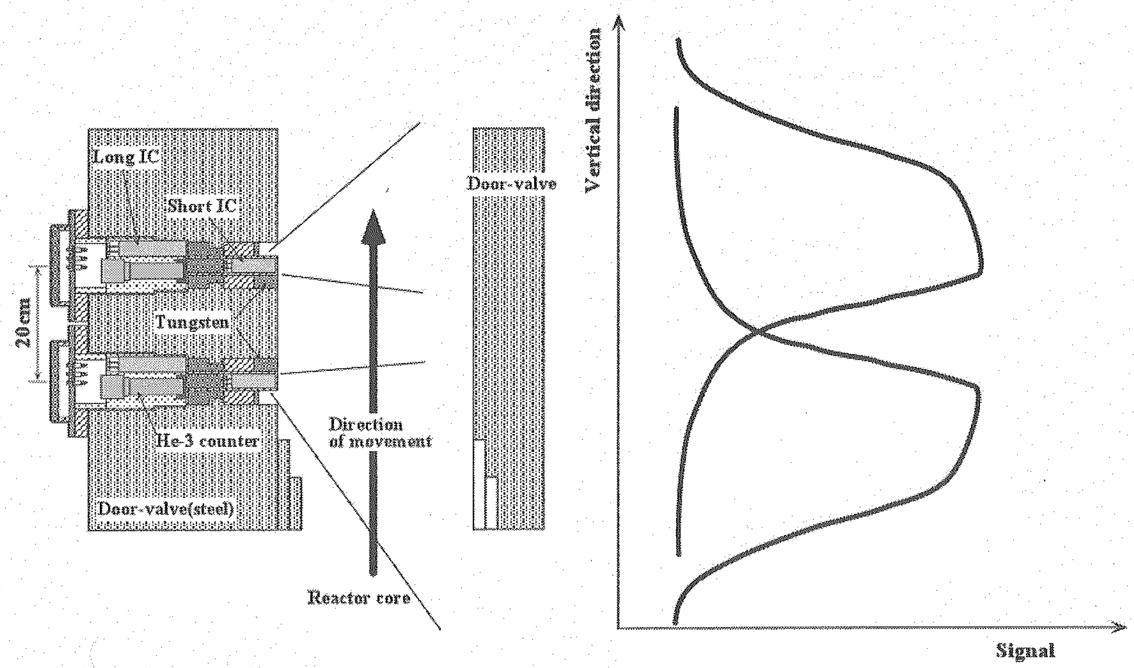

Fig. 3.5 Expected UFFM signal profile during spent fuel block transferring in door-valve

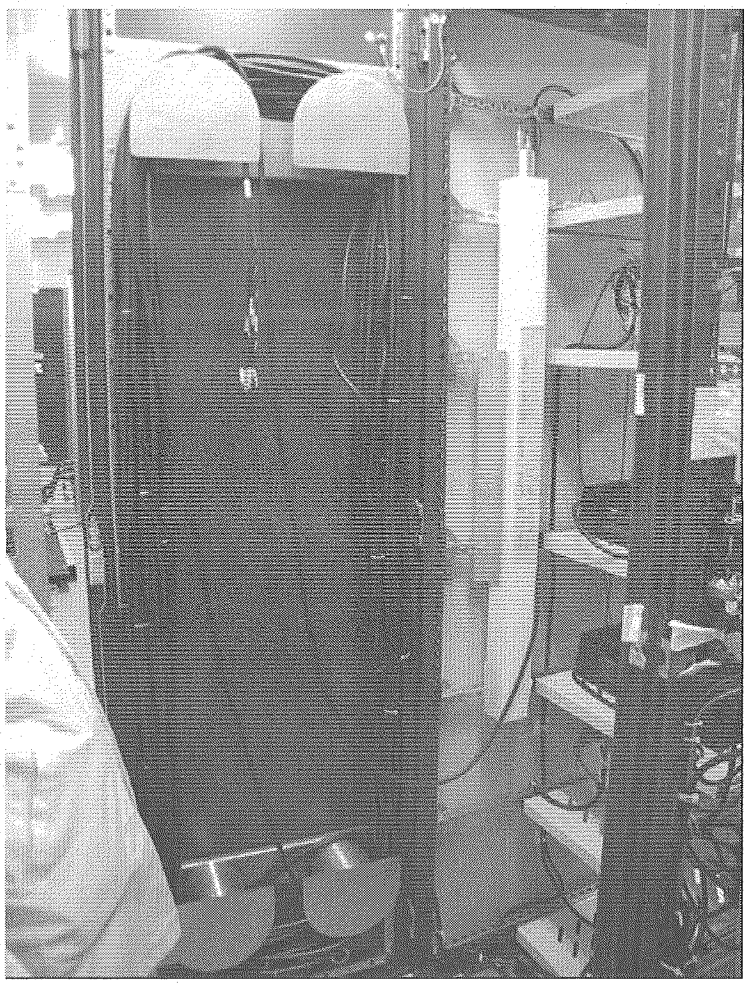

Fig. 3.6 Long He-3 counter inside the cabinet

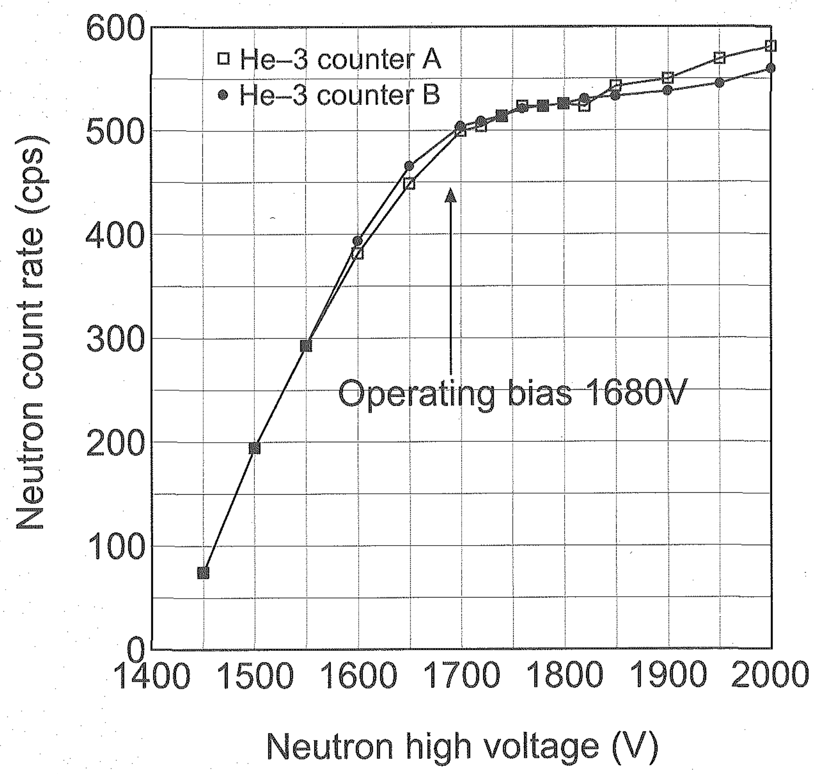

Fig. 4.1 Plateau curve of He-3 counter

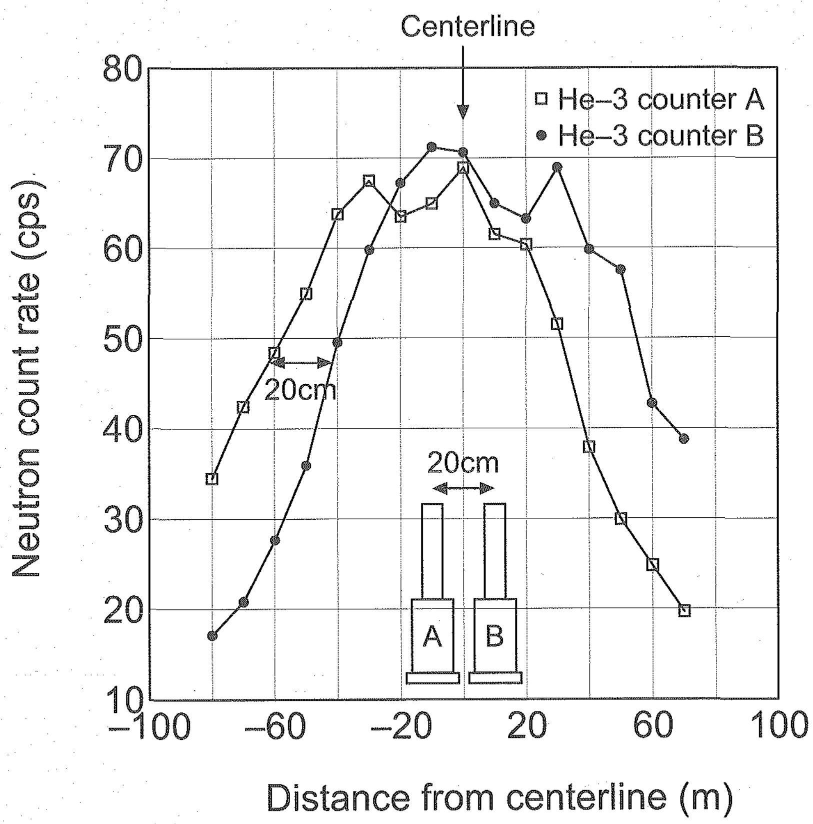

Fig. 4.2 Response profiles for He-3 counter when Cf neutron source is moved

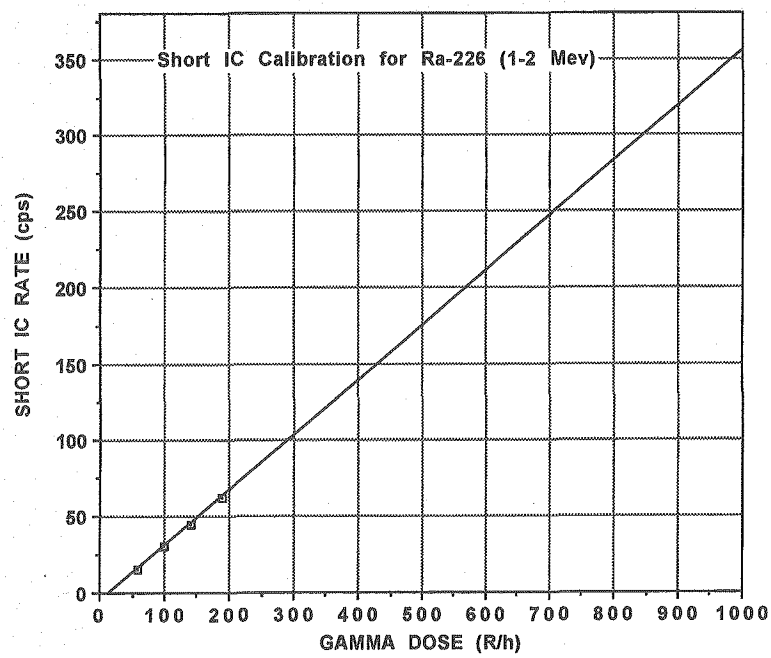

Fig. 4.3 The IC gamma response as a function of distance from the 1500 R/h ^{226}Ra gamma-ray source

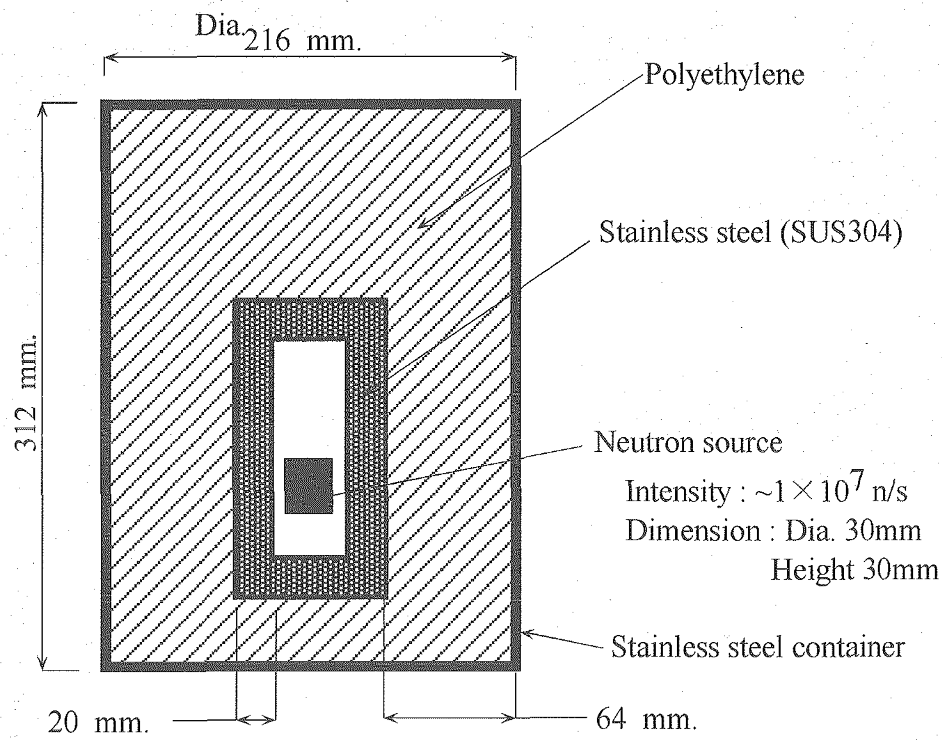

Fig. 4.4 Schematic cross-sectional view of Am-Be neutron source used in profile measurement

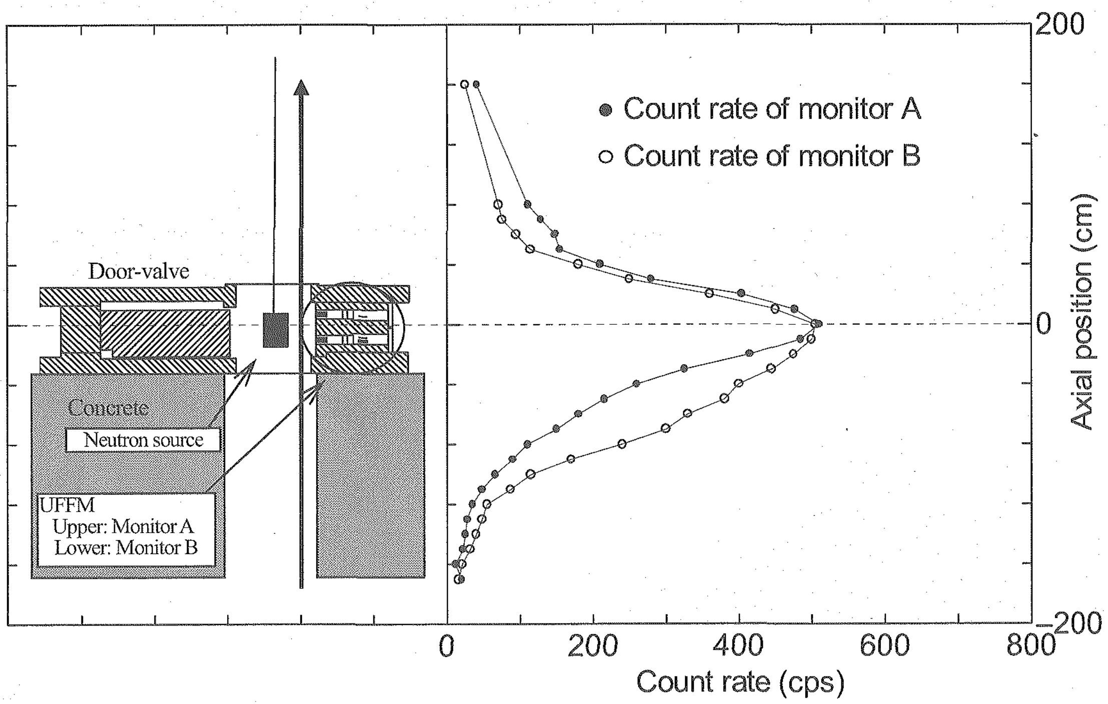

Fig. 4.5 Response profile of He-3 counter to vertical movement of Am-Be neutron source

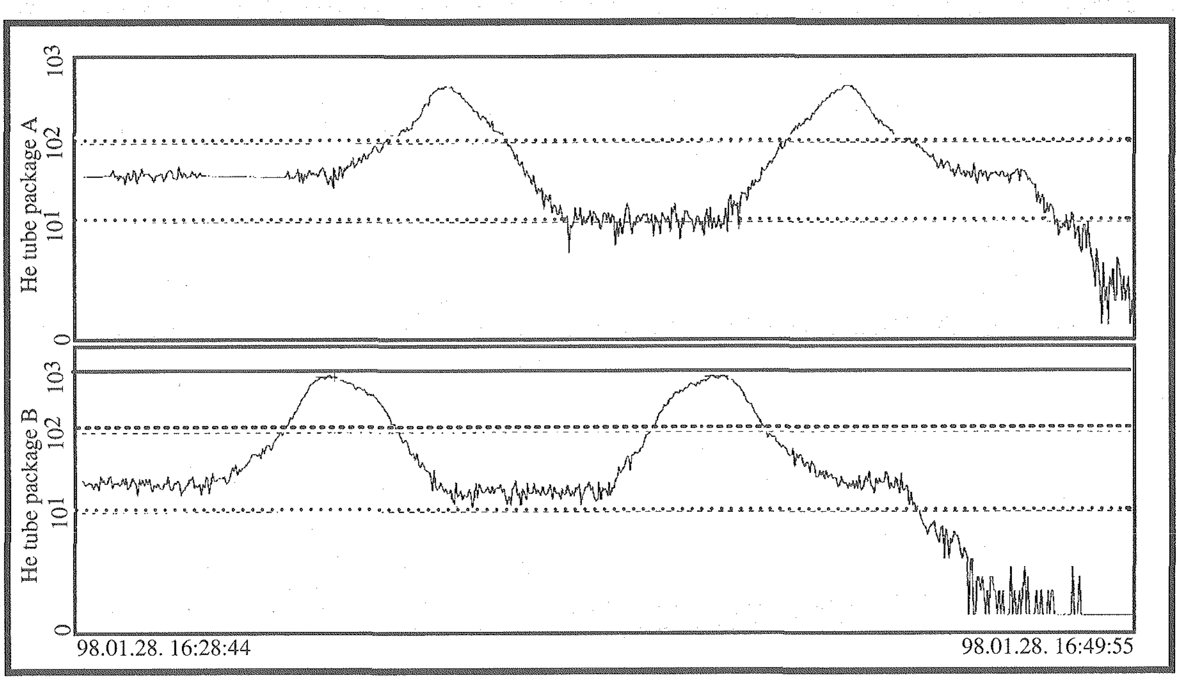

Fig. 4.6 Change of continuous neutron signal during vertical movement of neutron source

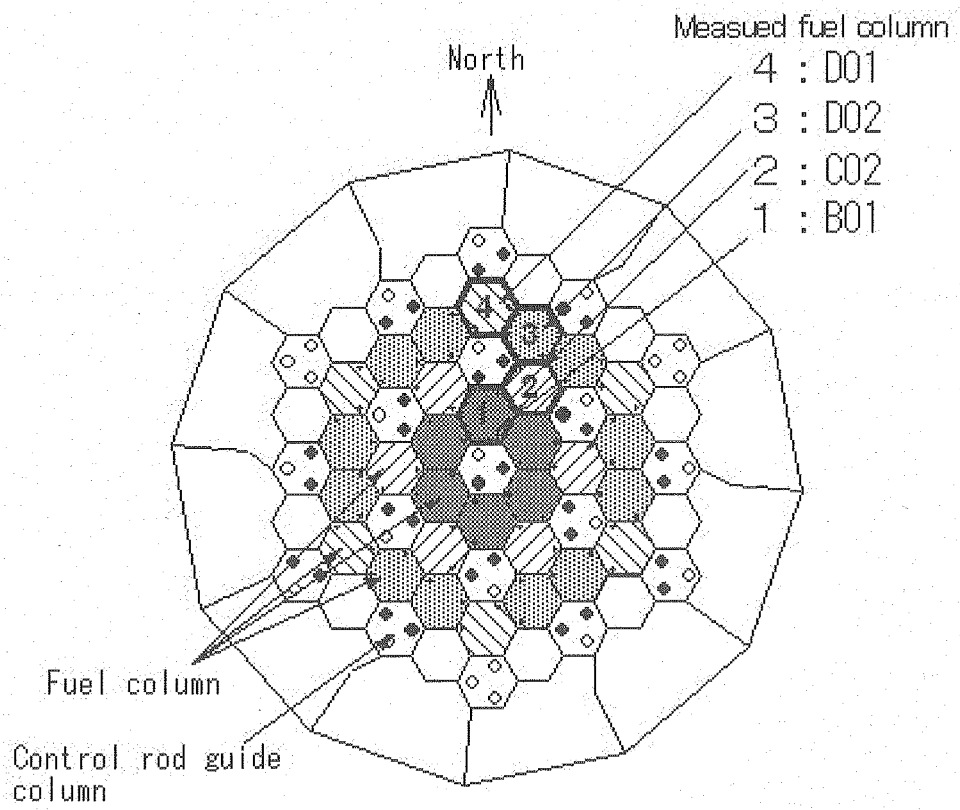

Fig. 4.7 HTTR core diagram indicating the locations of the measured columns

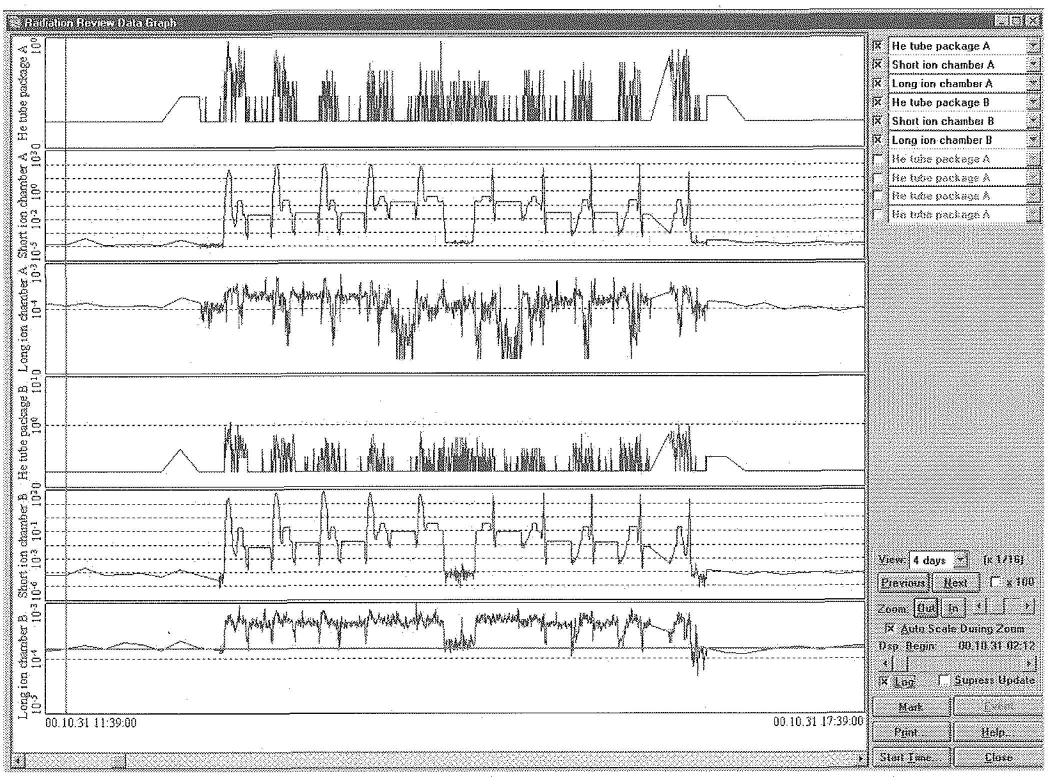

Fig. 4.8 Response from all detectors to 10 individual fuel movements (5 out, 5 in) in reference number 1 (Column B01)

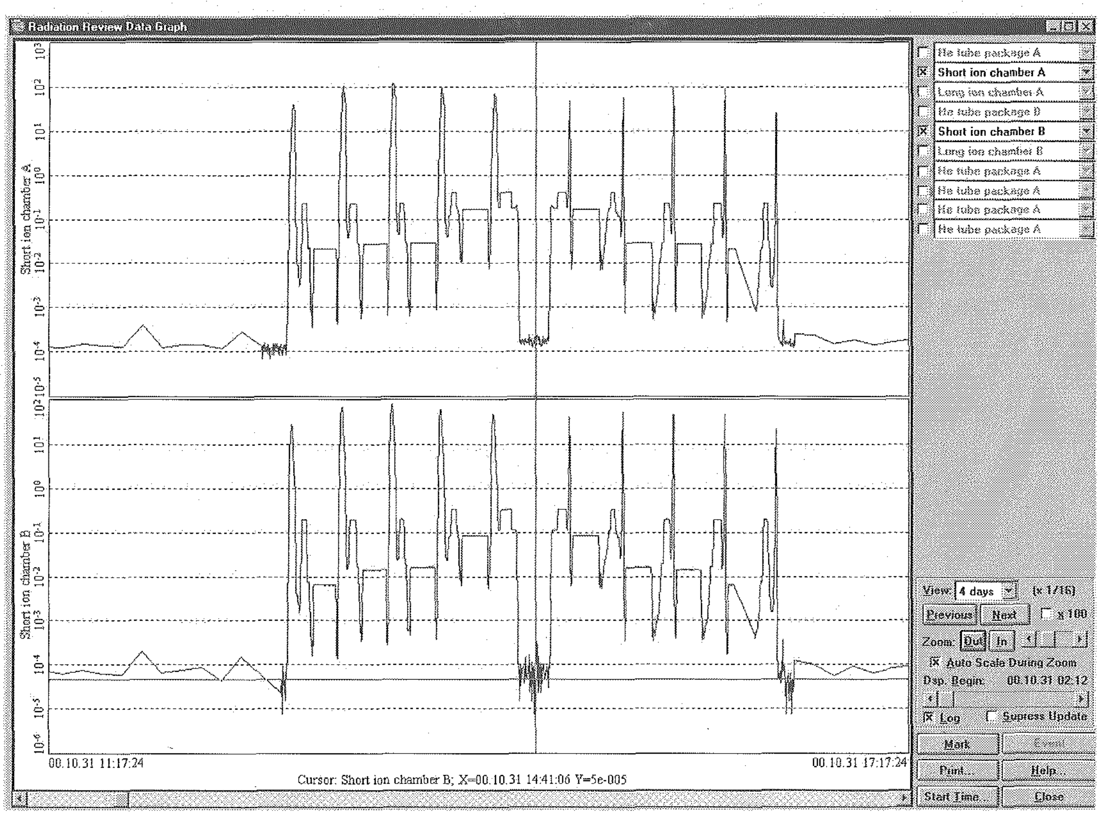

Fig. 4.9 Response from the short IC's to 10 individual fuel movements in reference number 1 (Column B01)

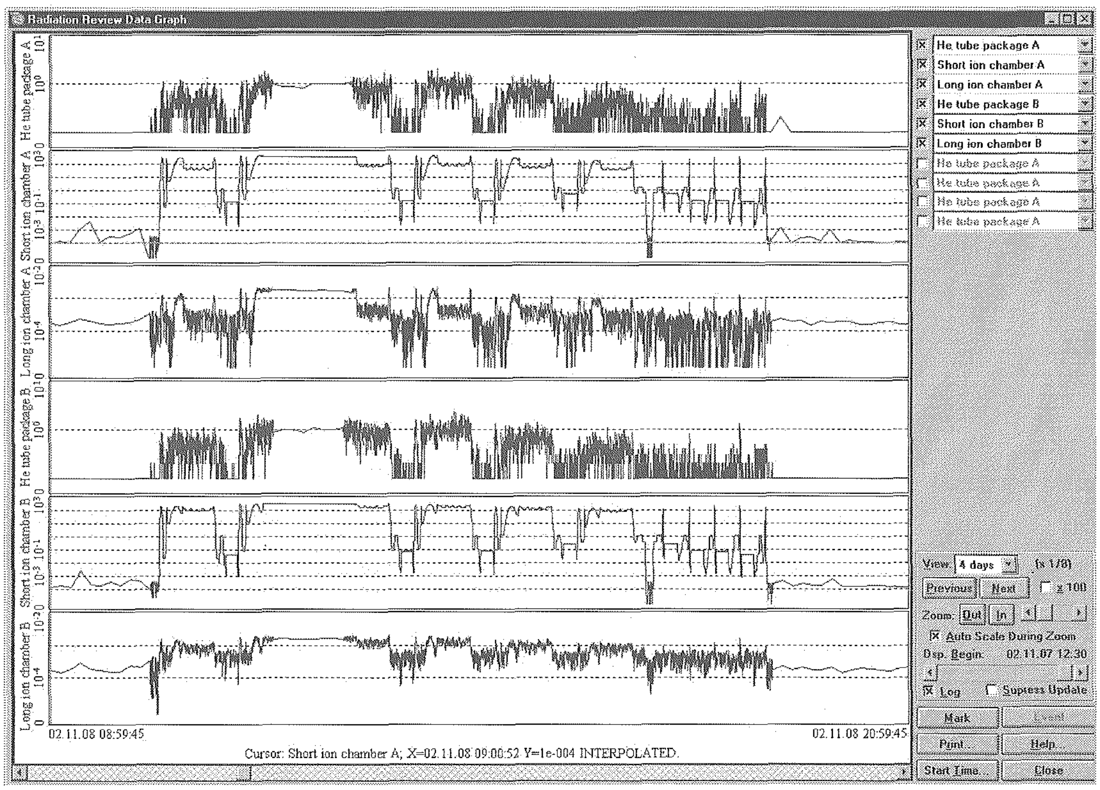

Fig. 4.10 Response from all detectors to 10 individual fuel movements in reference number 11 (Column B01)

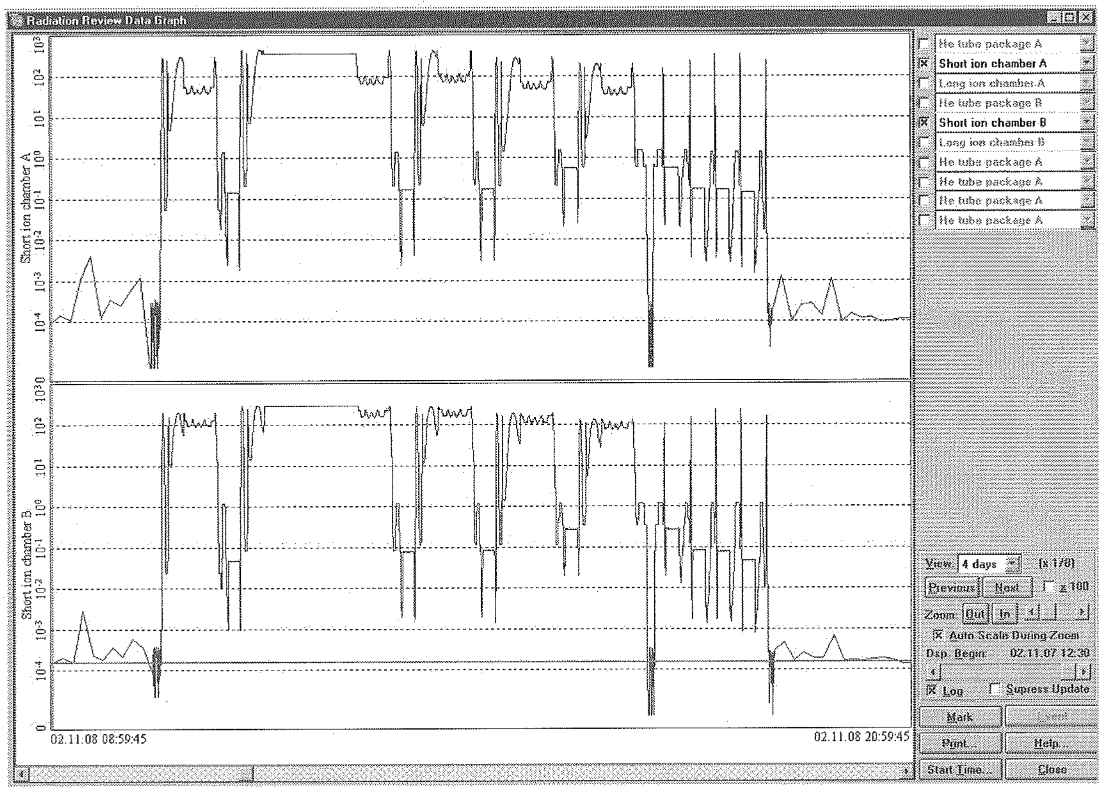

Fig. 4.11 Response from the short IC's to 10 individual fuel movements in reference number 11 (Column B01)

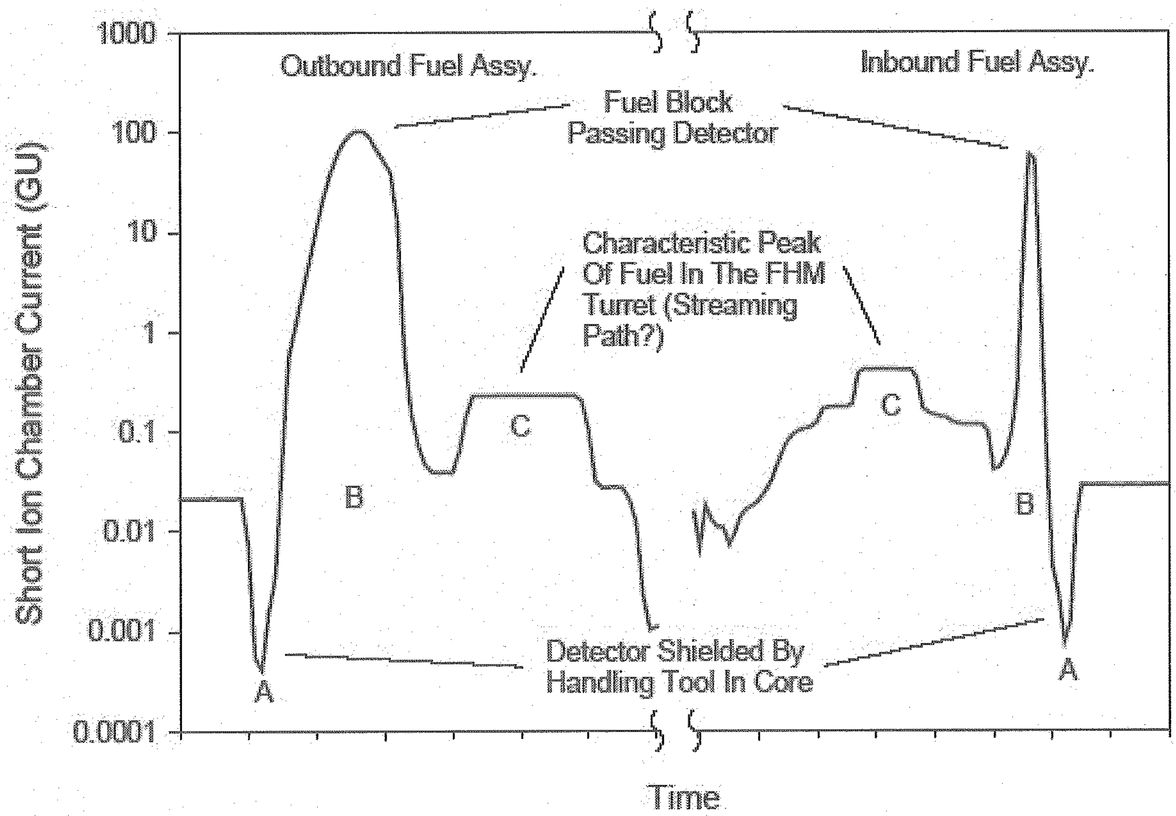

Fig. 4.12 Peak shape patterns for removal and replacement of fuel blocks

国際単位系（SI）

表１．SI 基本単位

基本量	SI 基本単位	
	名称	記号
長さ	メートル	m
質量	キログラム	kg
時間	秒	s
電流	アンペア	A
熱力学温度	ケルビン	K
物質量	モル	mol
光度	カンデラ	cd

表２．基本単位を用いて表されるSI組立単位の例

組立量	SI 基本単位	
	名称	記号
面積	平方メートル	m^2
体積	立法メートル	m^3
速さ，速度	メートル毎秒	m/s
加速度	メートル毎秒毎秒	m/s^2
波数	毎メートル	m-1
密度（質量密度）	キログラム毎立法メートル	kg/m^3
質量体積（比体積）	立法メートル毎キログラム	m^3/kg
電流密度	アンペア毎平方メートル	A/m^2
磁界の強さ	アンペア毎メートル	A/m
（物質量の）濃度	モル毎立方メートル	mol/m^3
輝度	カンデラ毎平方メートル	cd/m^2
屈折率	（数の）1	1

表５．SI 接頭語

乗数	接頭語	記号	乗数	接頭語	記号
10^{24}	ヨタ	Y	10^{-1}	デシ	d
10^{21}	ゼタ	Z	10^{-2}	センチ	c
10^{18}	エクサ	E	10^{-3}	ミリ	m
10^{15}	ペタ	P	10^{-6}	マイクロ	μ
10^{12}	テラ	T	10^{-9}	ナノ	n
10^{9}	ギガ	G	10^{-12}	ピコ	p
10^{6}	メガ	M	10^{-15}	フェムト	f
10^{3}	キロ	k	10^{-18}	アト	a
10^{2}	ヘクト	h	10^{-21}	ゼプト	z
10^{1}	デカ	da	10^{-24}	ヨクト	y

表３．固有の名称とその独自の記号で表されるSI組立単位

組立量	SI 組立単位			
	名称	記号	他のSI単位による表し方	SI基本単位による表し方
平面角	ラジアン[(a)]	rad		$m \cdot m^{-1}=1^{(b)}$
立体角	ステラジアン[(a)]	$sr^{(c)}$		$m^2 \cdot m^{-2}=1^{(b)}$
周波数	ヘルツ	Hz		s^{-1}
力	ニュートン	N		$m \cdot kg \cdot s^{-2}$
圧力，応力	パスカル	Pa	N/m^2	$m^{-1} \cdot kg \cdot s^{-2}$
エネルギー，仕事，熱量	ジュール	J	N・m	$m^2 \cdot kg \cdot s^{-2}$
工率，放射束	ワット	W	J/s	$m^2 \cdot kg \cdot s^{-3}$
電荷，電気量	クーロン	C		s・A
電位差（電圧），起電力	ボルト	V	W/A	$m^2 \cdot kg \cdot s^{-3} \cdot A^{-1}$
静電容量	ファラド	F	C/V	$m^{-2} \cdot kg^{-1} \cdot s^4 \cdot A^2$
電気抵抗	オーム	Ω	V/A	$m^2 \cdot kg \cdot s^{-3} \cdot A^{-2}$
コンダクタンス	ジーメンス	S	A/V	$m^{-2} \cdot kg^{-1} \cdot s^3 \cdot A^2$
磁束	ウエーバ	Wb	V・s	$m^2 \cdot kg \cdot s^{-2} \cdot A^{-1}$
磁束密度	テスラ	T	Wb/m^2	$kg \cdot s^{-2} \cdot A^{-1}$
インダクタンス	ヘンリー	H	Wb/A	$m^2 \cdot kg \cdot s^{-2} \cdot A^{-2}$
セルシウス温度	セルシウス度[(d)]	℃		K
光束	ルーメン	lm	$cd \cdot sr^{(c)}$	$m^2 \cdot m^{-2} \cdot cd=cd$
照度	ルクス	lx	lm/m^2	$m^2 \cdot m^{-4} \cdot cd=m^{-2} \cdot cd$
（放射性核種の）放射能	ベクレル	Bq		s^{-1}
吸収線量，質量エネルギー分与，カーマ	グレイ	Gy	J/kg	$m^2 \cdot s^{-2}$
線量当量，周辺線量当量，方向性線量当量，個人線量当量，組織線量当	シーベルト	Sv	J/kg	$m^2 \cdot s^{-2}$

(a)ラジアン及びステラジアンの使用は、同じ次元であっても異なった性質をもった量を区別するときの組立単位の表し方として利点がある。組立単位を形作るときのいくつかの用例は表４に示されている。
(b)実際には、使用する時には記号rad及びsrが用いられるが、習慣として組立単位としての記号“1”は明示されない。
(c)測光学では、ステラジアンの名称と記号srを単位の表し方の中にそのまま維持している。
(d)この単位は、例としてミリセルシウス度m℃のようにSI接頭語を伴って用いても良い。

表４．単位の中に固有の名称とその独自の記号を含むSI組立単位の例

組立量	SI 組立単位		
	名称	記号	SI 基本単位による表し方
粘度	パスカル秒	Pa・s	$m^{-1} \cdot kg \cdot s^{-1}$
力のモーメント	ニュートンメートル	N・m	$m^2 \cdot kg \cdot s^{-2}$
表面張力	ニュートン毎メートル	N/m	$kg \cdot s^{-2}$
角速度	ラジアン毎秒	rad/s	$m \cdot m^{-1} \cdot s^{-1}=s^{-1}$
角加速度	ラジアン毎平方秒	rad/s^2	$m \cdot m^{-1} \cdot s^{-2}=s^{-2}$
熱流密度，放射照度	ワット毎平方メートル	W/m^2	$kg \cdot s^{-3}$
熱容量，エントロピー	ジュール毎ケルビン	J/K	$m^2 \cdot kg \cdot s^{-2} \cdot K^{-1}$
質量熱容量（比熱容量），質量エントロピー	ジュール毎キログラム毎ケルビン	J/(kg・K)	$m^2 \cdot s^{-2} \cdot K^{-1}$
質量エネルギー（比エネルギー）	ジュール毎キログラム	J/kg	$m^2 \cdot s^{-2} \cdot K^{-1}$
熱伝導率	ワット毎メートル毎ケルビン	W/(m・K)	$m \cdot kg \cdot s^{-3} \cdot K^{-1}$
体積エネルギー	ジュール毎立方メートル	J/m^3	$m^{-1} \cdot kg \cdot s^{-2}$
電界の強さ	ボルト毎メートル	V/m	$m \cdot kg \cdot s^{-3} \cdot A^{-1}$
体積電荷	クーロン毎立方メートル	C/m^3	$m^{-3} \cdot s \cdot A$
電気変位	クーロン毎平方メートル	C/m^2	$m^{-2} \cdot s \cdot A$
誘電率	ファラド毎メートル	F/m	$m^{-3} \cdot kg^{-1} \cdot s^4 \cdot A^2$
透磁率	ヘンリー毎メートル	H/m	$m \cdot kg \cdot s^{-2} \cdot A^{-2}$
モルエネルギー	ジュール毎モル	J/mol	$m^2 \cdot kg \cdot s^{-2} \cdot mol^{-1}$
モルエントロピー，モル熱容量	ジュール毎モル毎ケルビン	J/(mol・K)	$m^2 \cdot kg \cdot s^{-2} \cdot K^{-1} \cdot mol^{-1}$
照射線量（Ｘ線及びγ線）	クーロン毎キログラム	C/kg	$kg^{-1} \cdot s \cdot A$
吸収線量率	グレイ毎秒	Gy/s	$m^2 \cdot s^{-3}$
放射強度	ワット毎ステラジアン	W/sr	$m^4 \cdot m^{-2} \cdot kg \cdot s^{-3}=m^2 \cdot kg \cdot s^{-3}$
放射輝度	ワット毎平方メートル毎ステラジアン	$W/(m^2 \cdot sr)$	$m^2 \cdot m^{-2} \cdot kg \cdot s^{-3}=kg \cdot s^{-3}$

表６．国際単位系と併用されるが国際単位系に属さない単位

名称	記号	SI 単位による値
分	min	1 min=60s
時	h	1h =60 min=3600 s
日	d	1 d=24 h=86400 s
度	°	1° =(π/180) rad
分	’	1’ =(1/60)° =(π/10800) rad
秒	”	1” =(1/60)’ =(π/648000) rad
リットル	l、L	$1l=1\ dm^3=10^{-3}m^3$
トン	t	$1t=10^3$ kg
ネーパ	Np	1Np=1
ベル	B	1B=(1/2)ln10(Np)

表７．国際単位系と併用されこれに属さない単位でSI単位で表される数値が実験的に得られるもの

名称	記号	SI 単位であらわされる数値
電子ボルト	eV	$1eV=1.60217733(49)\times10^{-19}J$
統一原子質量単位	u	$1u=1.6605402(10)\times10^{-27}kg$
天文単位	ua	$1ua=1.49597870691(30)\times10^{11}m$

表８．国際単位系に属さないが国際単位系と併用されるその他の単位

名称	記号	SI 単位であらわされる数値
海里		１海里=1852m
ノット		１ノット=１海里毎時=(1852/3600)m/s
アール	a	$1\,a=1\ dam^2=10^2m^2$
ヘクタール	ha	$1\,ha=1\ hm^2=10^4m^2$
バール	bar	$1\,bar=0.1MPa=100kPa=1000hPa=10^5Pa$
オングストローム	Å	$1\,Å=0.1nm=10^{-10}m$
バーン	b	$1\,b=100fm^2=10^{-28}m^2$

表９．固有の名称を含むCGS組立単位

名称	記号	SI 単位であらわされる数値
エルグ	erg	$1\ erg=10^{-7}\ J$
ダイン	dyn	$1\ dyn=10^{-5}N$
ポアズ	P	$1\ P=1\ dyn \cdot s/cm^2=0.1Pa \cdot s$
ストークス	St	$1\ St\ =1cm^2/s=10^{-4}m^2/s$
ガウス	G	1 G ˆ10^{-4}T
エルステッド	Oe	1 Oe ˆ(1000/4π)A/m
マクスウェル	Mx	1 Mx ˆ10^{-8}Wb
スチルブ	sb	$1\ sb\ =1cd/cm^2=10^4cd/m^2$
ホト	ph	$1\ ph=10^4lx$
ガル	Gal	$1\ Gal\ =1cm/s^2=10^{-2}m/s^2$

表10．国際単位に属さないその他の単位の例

名称	記号	SI 単位であらわされる数値
キュリー	Ci	$1\ Ci=3.7\times10^{10}Bq$
レントゲン	R	$1\ R\ =2.58\times10^{-4}C/kg$
ラド	rad	$1\ rad=1cGy=10^{-2}Gy$
レム	rem	$1\ rem=1\ cSv=10^{-2}Sv$
X線単位		$1X\ unit=1.002\times10^{-4}nm$
ガンマ	γ	$1\gamma=1\ nT=10^{-9}T$
ジャンスキー	Jy	$1\ Jy=10^{-26}W \cdot m^{-2} \cdot Hz^{-1}$
フェルミ		$1\ fermi=1\ fm=10^{-15}m$
メートル系カラット		$1\ metric\ carat\ =\ 200\ mg\ =\ 2\times10^{-4}kg$
トル	Torr	1 Torr = (101 325/760) Pa
標準大気圧	atm	1 atm = 101 325 Pa
カロリー	cal	
ミクロン	μ	$1\ \mu=1\mu m=10^{-6}m$

（第７版，1998年改訂）